
LATTICE DYNAMICS
AND PHASE TRANSITIONS

Calorimetric and X-ray Diffraction Studies of the $(\text{NH}_4)_3\text{WO}_3\text{F}_3$ and $(\text{NH}_4)_3\text{TiOF}_5$ Perovskite-Like Oxyfluorides

I. N. Flerov*, M. V. Gorev*, V. D. Fokina*, A. F. Bovina*, and N. M. Laptash**

*Kirensky Institute of Physics, Siberian Division, Russian Academy of Sciences,
Akademgorodok, Krasnoyarsk, 660036 Russia

e-mail: flerov@ksc.krasn.ru

**Institute of Chemistry, Far East Division, Russian Academy of Sciences,
pr. Stoletiya Vladivostoka 159, Vladivostok, 690022 Russia

Received July 15, 2003

Abstract—The heat capacity and unit cell parameters of the $(\text{NH}_4)_3\text{WO}_3\text{F}_3$ and $(\text{NH}_4)_3\text{TiOF}_5$ perovskite-like oxyfluorides were measured in the temperature interval from 80 to 300 K; the existence of two and one phase transitions in these compounds, respectively, was demonstrated, and their thermodynamic parameters were determined. The effect of a hydrostatic pressure of up to 0.5 GPa on the phase transition temperatures was studied. Triple points and high-pressure phases were found in the T vs. p diagrams. An analysis of entropy changes suggests that all the structural transformations revealed are associated with the ordering of structural blocks.
© 2004 MAIK “Nauka/Interperiodica”.

1. INTRODUCTION

The perovskite-like fluoride compounds with general chemical formula $A_3M^{3+}F_6$ have cubic symmetry with space group $Fm\bar{3}m$ ($Z = 4$) in the high-temperature phase and belong to the cryolite–elpasolite family [1]. It was shown in [2] that the original cubic symmetry persists under partial substitution of oxygen for the fluorine ions, i.e., in $A_3MO_xF_{6-x}$ compounds (with the value of x depending on the actual valence of the central M atom), because the atoms of fluorine and oxygen are distributed at random over the lattice. The point symmetry of the O_xF_{6-x} octahedra was found from IR and Raman spectra to be lower than cubic, C_{4v} (for $x = 1$) and C_{2v} (for $x = 3$) [3, 4].

The perovskite-like oxyfluorides with atomic cations, like the related fluorides, have a distorted structure at room temperature and undergo, with increasing temperature, single or sequential structural transformations [5, 6]. Our present knowledge of the structure of the original and distorted phases of the oxyfluorides is inadequate. The symmetry of the cubic phase has been refined only for $\text{Rb}_2\text{KMoO}_3\text{F}_3$ [7] solely using a model that assumes the oxygen and fluorine atoms to be distributed over the $24e$ positions, for which the thermal vibration anisotropy was found to be essential. A variety of symmetries of the low-temperature phase (which exists, for instance, in $\text{K}_3\text{MoO}_3\text{F}_3$ at room temperature and is a result of two successive phase transitions) have been proposed, from trigonal [8] and orthorhombic [2] to monoclinic [9]. The phase transitions occurring in

$A_3M^{3+}F_6$ and $A_3MO_xF_{6-x}$ are different in nature [1, 3]. The fluorides in distorted phases are ferroelastics, whereas the oxyfluorides undergo ferroelectric and ferroelastic transformations. Substitution of a spherical cation with the tetrahedral ammonium ion in fluorides brings about a noticeable lowering of the temperature at which the cubic phase loses stability. On the other hand, the nonsphericity of cation A may initiate additional disorder resulting from disordering of the tetrahedra in the $4b$ and/or $8c$ positions [1]. In connection with the low symmetry of the fluorine–oxygen octahedra, it was unclear how such effects would become manifest in the perovskite-like oxyfluorides.

Information on phase transitions in ammonium oxyfluorides has thus far been lacking. We performed a synthesis and investigation of the $(\text{NH}_4)_3\text{WO}_3\text{F}_3$ and $(\text{NH}_4)_3\text{TiOF}_5$ compounds to look for and study their possible phase transitions. For this purpose, we used differential scanning calorimetry, x-ray diffraction, adiabatic calorimetry, and differential thermal analysis (DTA) under pressure.

2. SAMPLE PREPARATION AND TRIAL EXPERIMENTS

The ammonium oxyfluorides $(\text{NH}_4)_3\text{WO}_3\text{F}_3$ and $(\text{NH}_4)_3\text{TiOF}_5$ were prepared from hot $(\text{NH}_4)_2\text{WO}_2\text{F}_4$ and $(\text{NH}_4)_2\text{TiF}_6$ solutions with excess NH_4F , with subsequent gradual addition of an NH_4OH solution to pH = 8 (until the first signs of precipitation of a white sediment appear). Such fast crystallization produces small, transparent, colorless crystals of octahedral

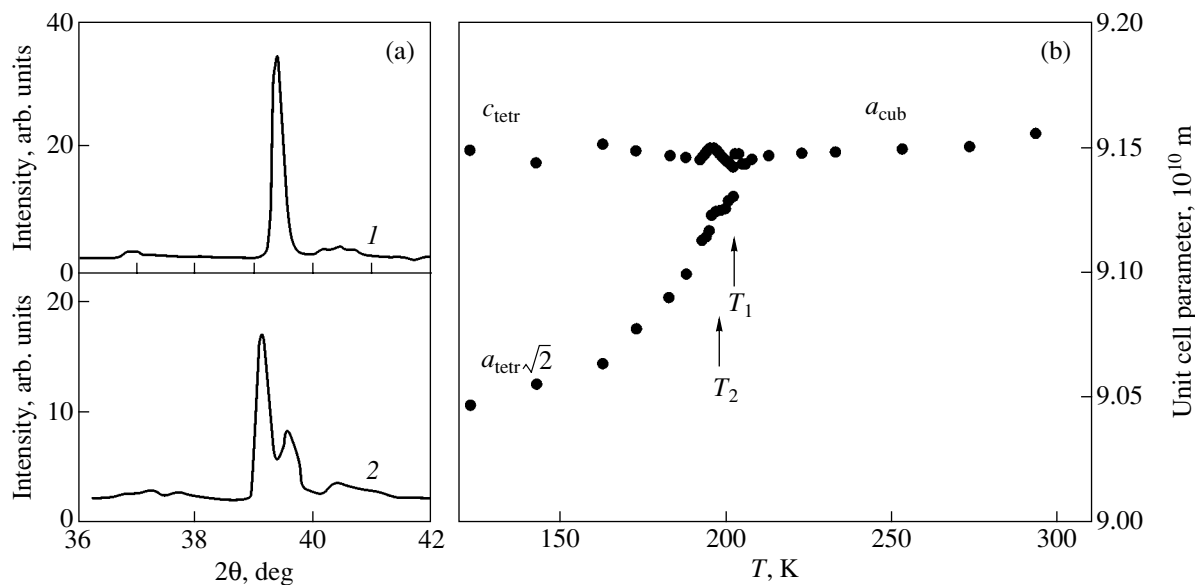


Fig. 1. X-ray characterization of $(\text{NH}_4)_3\text{WO}_3\text{F}_3$: (a) (400) reflection at (1) 293 and (2) 123 K and (b) temperature dependence of the unit cell parameters.

shape with an edge of about 5 μm . Following separation of the crystalline precipitate from the mother growth solution, larger octahedra crystallized under slow evaporation in air with edges about 40 μm long.

At room temperature, both cryolites were found to have cubic symmetry ($Fm\bar{3}m$, $Z = 4$) with the unit cell parameters $a_0 = 0.9156$ nm for $(\text{NH}_4)_3\text{WO}_3\text{F}_3$ and 0.9113 nm for $(\text{NH}_4)_3\text{TiOF}_5$. No peaks associated with residual impurities of the starting components or foreign phases were observed in the diffraction patterns.

The preliminary thermophysical studies of the two cryolites were performed using differential scanning microcalorimetry (DSM). We measured the heat capacity of the samples of the compounds prepared by fast and slow crystallization. The measurements were conducted in the temperature range from 120 to 330 K in heating and cooling runs at a rate of 8 K/min. The sample mass was about 0.1–0.2 g. The heat capacity of the $(\text{NH}_4)_3\text{WO}_3\text{F}_3$ oxyfluoride was found to behave anomalously under heating; namely, it revealed a sharp peak with a maximum at the temperature $T_1 = 201 \pm 1$ K. A shoulder was observed in the rising part of the peak at $T_2 \approx 199$ K. A conjecture was put forward that this compound undergoes a sequence of two phase transitions. Measurements carried out under cooling provided supportive evidence of this conjecture; namely, the heat capacity peak split in two because of a difference in hysteresis of the phase transition temperatures ($\delta T_1 \approx 3$ K, $\delta T_2 \approx 5$ K). Because the intermediate phase exists in a very narrow temperature interval, we could determine only the total enthalpy change, $\Sigma\Delta H_i = 3200 \pm 320$ J/mol, associated with the phase transition sequence.

In the $(\text{NH}_4)_3\text{TiOF}_5$ compound, DSM revealed only one phase transition at $T_0 = 270 \pm 1$ K with a temperature hysteresis $\delta T_0 \approx 11$ K. The enthalpy change for this compound was found to be considerably larger, $\Delta H_0 = 5000 \pm 500$ J/mol.

The calorimetric data obtained with DSM on samples prepared in various crystallization regimes are in satisfactory agreement within the error of measurement for both compounds.

To verify that the anomalies in the heat capacity are indeed related to structural transformations, we carried out x-ray studies of both compounds within a broad temperature range. The structural distortion of tungsten oxyfluoride was reflected in the broadening and splitting of the $(h00)$ and $(hk0)$ reflections setting in at T_1 . Figure 1a shows a characteristic transformation of the (400) reflection. The pattern of the splitting did not change under a further decrease in temperature. The data obtained were insufficient for determining the symmetry of the distorted phases; therefore, Fig. 1b displays the temperature dependence of the parameters of a pseudotetragonal cell with the following relations:

$a_{\text{tet}} \approx a_{\text{cub}}/\sqrt{2}$ and $c_{\text{tet}} \approx a_{\text{cub}}$. The behavior of the parameters exhibits two singular points at the temperatures T_1 and T_2 , which can be identified with the phase transitions revealed by DSM in tungsten oxyfluoride.

The existence of a phase transition in $(\text{NH}_4)_3\text{TiOF}_5$ at 270 K was also confirmed by x-ray diffraction. A comparison of the x-ray diffractograms of this compound obtained at room temperature and 123 K (Fig. 2a) suggests, however, that the phase transition, besides causing the reflection splitting for $T < T_0$, gives rise to the appearance of additional peaks signaling the presence of a superstructure. One may thus conclude

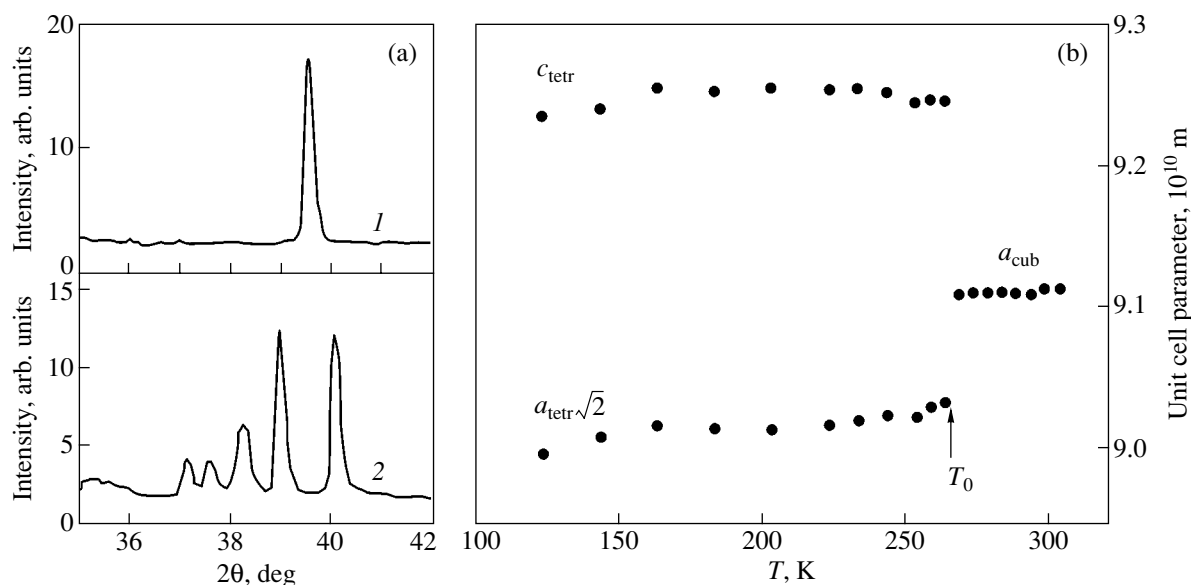


Fig. 2. X-ray characterization of $(\text{NH}_4)_3\text{TiOF}_5$: (a) (400) reflection at (1) 293 and (2) 123 K and (b) temperature dependence of the unit cell parameters.

that the symmetry of the low-temperature phase in titanium oxyfluoride is different from that of the distorted phases in the tungsten compound. Nevertheless, most of the lines in the powder x-ray diffraction pattern of $(\text{NH}_4)_3\text{TiOF}_5$ can also be indexed with the use of a tetragonal pseudocell. The $a_i(T)$ relation is plotted in Fig. 2b. The abrupt change in the cell parameters and the sharp heat capacity peak suggest that the structural transformation in the $(\text{NH}_4)_3\text{TiOF}_5$ compound is a clearly pronounced first-order phase transition.

3. HEAT CAPACITY MEASUREMENTS

The enthalpy change at the phase transition derived from DSM measurements is quite often found to be an underestimate, particularly in studies of transformations far from the tri-critical point, because this method has a relatively low sensitivity to pretransition phenomena occurring in the heat capacity behavior. Therefore, to refine the thermodynamic parameters of the phase transitions revealed in the compounds under study, we carried out comprehensive measurements of the temperature dependence of the heat capacity of $(\text{NH}_4)_3\text{WO}_3\text{F}_3$ and $(\text{NH}_4)_3\text{TiOF}_5$ with an adiabatic calorimeter within the temperature range from 80 to 300 K.

The samples to be studied, with a mass of about 1 g, were hermetically sealed in an indium container in a helium environment. The measurements were conducted in a discrete ($\Delta T = 2.5\text{--}4.0$ K) and a continuous ($dT/dt = 0.14$ K/min) heating mode. The method of quasi-static thermograms with average heating and cooling rates $|dT/dt| \approx 0.04$ K/min was employed in the immediate vicinity of the phase transitions. The temperatures were measured with a platinum resistance thermometer.

Figure 3a displays the temperature dependence of the heat capacity of the $(\text{NH}_4)_3\text{WO}_3\text{F}_3$ compound measured over a broad temperature range. The region of the anomalies, which was studied from thermograms, is shown in more detail in Fig. 3b. Two heat capacity peaks were found to exist at temperatures $T_1 = 200.1 \pm 0.1$ K and $T_2 = 198.5 \pm 0.1$ K. The temperature hysteresis was $\delta T_1 = 2.2$ K and $\delta T_2 = 5.1$ K. The results obtained are in satisfactory agreement with the DSM measurements. When processing adiabatic calorimeter data, we likewise did not succeed in separating the heat

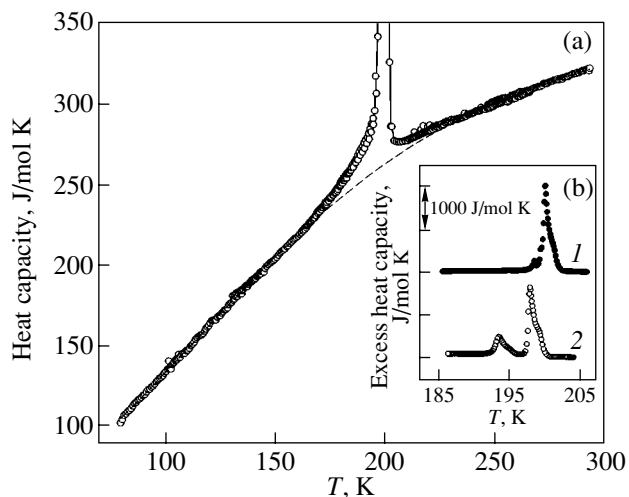


Fig. 3. Temperature dependence (a) of the heat capacity of $(\text{NH}_4)_3\text{WO}_3\text{F}_3$ over a broad temperature range and (b) of the excess heat capacity at the phase transitions measured (1) under heating and (2) under cooling. The dashed line represents the lattice heat capacity.

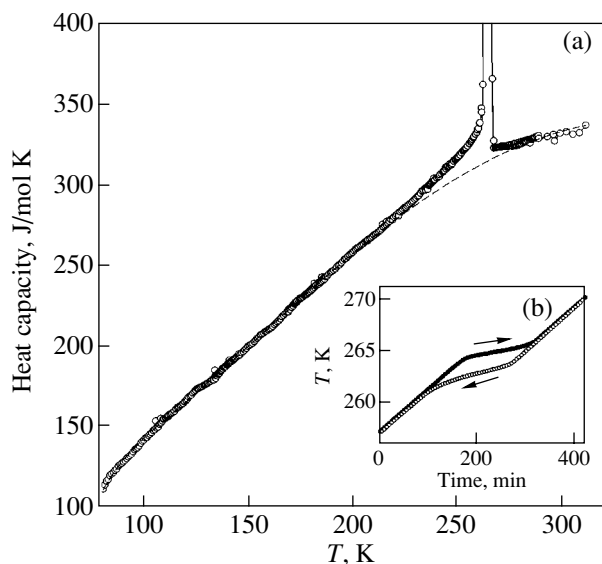


Fig. 4. (a) Temperature dependence of the heat capacity of $(\text{NH}_4)_3\text{TiOF}_5$ over a broad temperature range; The dashed line represents the lattice heat capacity. (b) Thermograms obtained in the heating and cooling modes near T_0 .

capacity anomalies associated with the phase transition sequence. Therefore, we calculated the total enthalpy change in the two phase transitions by integrating the excess heat capacity $\Delta C_p(T)$ over temperature, derived by subtracting the lattice contribution from the total heat capacity. The temperature dependence of the regular heat capacity, obtained through polynomial fitting of experimental data outside the phase transition region, is shown in Fig. 3a with a dashed line. The average scatter of experimental data from the smoothed curve did not exceed 1%. By properly varying the temperature intervals within which the anomalous heat capacity was cut out, it was established that the anomaly exists within a broad temperature region below $(T_1 - 40 \text{ K})$ and above $(T_1 + 29 \text{ K})$ the temperature of the phase transition from the cubic phase. It is obvious, however, that the excess heat capacity near the temperatures of the transformations provides the main contribution to the enthalpy change. The calculated total enthalpy change was found to be $\Sigma\Delta H_i = 3370 \pm 250 \text{ J/mol}$. The total change in the enthalpy in the two phase transitions was found (by integrating the function $\Delta C_p(T)/T$ over temperature) to be $\Sigma\Delta S_i = 16.9 \pm 1.2 \text{ J/mol K}$.

The measured specific heat capacity of the $(\text{NH}_4)_3\text{TiOF}_5$ oxyfluoride is shown graphically in Fig. 4a. As in the DSM experiments, we observed one heat capacity anomaly. The refined phase transition temperature is $T_0 = 264.7 \pm 0.1 \text{ K}$. The anomalous heat capacity was isolated in a way similar to that used to analyze the heat capacity of the tungsten compound. The excess heat capacity of $(\text{NH}_4)_3\text{TiOF}_5$ also exists within a broad temperature region, from $(T_0 - 75 \text{ K})$ to $(T_0 + 25 \text{ K})$. The changes in the enthalpy and entropy were determined in the same way as was done for tung-

sten oxyfluoride, namely, by integrating the corresponding functions, $\Delta C_p(T)$ and $\Delta C_p(T)/T$, to yield $\Delta H_0 = 4820 \pm 250 \text{ J/mol}$ and $\Delta S_0 = 18.1 \pm 1.0 \text{ J/mol K}$.

Figure 4b presents thermograms obtained for the titanium compound under heating and cooling. Absorption of the latent heat of the transition during the sample heating was observed to occur in the interval $T_0 \pm 0.7 \text{ K}$. This yielded $\delta H_0 = 4200 \pm 220 \text{ J/mol}$ for the latent heat and $\delta S_0 = 15.4 \pm 0.8 \text{ J/mol K}$ for the entropy jump. The value of the temperature hysteresis, $\delta T_0 = 2.3 \text{ K}$, was found to be substantially smaller than that extracted from DSM experiments.

4. PHASE DIAGRAMS

Thus, both calorimetric and x-ray diffraction data suggest that $(\text{NH}_4)_3\text{WO}_3\text{F}_3$ undergoes, at atmospheric pressure, a sequence of phase transitions $G_0(Fm\bar{3}m) \rightarrow G_1 \rightarrow G_2$ and that $(\text{NH}_4)_3\text{TiOF}_5$ undergoes only one transformation, $G_0 \rightarrow G'_1$. The experience gained in investigating related fluorides [10, 11] gave us grounds to believe that the ammonium oxyfluorides could likewise turn out to be sensitive to external pressure.

The effect of external pressure on phase transition temperatures in both ammonium oxyfluorides was studied on samples prepared by fast crystallization. The transition temperature and its variation with pressure were measured by DTA. The sensor was a thermocouple fabricated by attaching copper wires with tin-lead solder to a germanium parallelepiped. A quartz bar was pasted as a reference to one junction of the thermocouple, and a small copper container with the substance to be measured, to the other junction. The sample mass was $\sim 0.1 \text{ g}$. A pressure of up to 0.5 GPa was produced in a cylinder-piston-type chamber connected to a multiplier. A mixture of transformer oil with pentane served as the pressure-transmitting medium. The pressure and temperature in the chamber were measured with a managanin resistance manometer and a copper-constantan thermocouple, with errors of $\pm 10^{-3} \text{ GPa}$ and $\pm 0.3 \text{ K}$, respectively. The position of the phase boundaries in the T vs. p diagrams was established under increasing and decreasing hydrostatic pressure.

Figure 5 presents a T vs. p phase diagram of $(\text{NH}_4)_3\text{WO}_3\text{F}_3$. At atmospheric pressure, the temperature dependence of the DTA signal exhibited only one anomaly. We did not observe a splitting of the peak associated with the $G_0 \rightarrow G_1 \rightarrow G_2$ sequence, most likely because the DTA is less sensitive than DSM, which reliably detected both transitions, as already mentioned, in the cooling run only. Unfortunately, the DTA method employed by us does not allow us to perform measurements in the cooling mode.

This pattern of the phase diagram suggests that the G_1 phase found in the $(\text{NH}_4)_3\text{WO}_3\text{F}_3$ cryolite at atmospheric pressure disappears rapidly with increasing pressure and that the phase boundary observed to exist

up to the pressure of the triple point revealed in the diagram should be identified with the $G_0 \rightarrow G_2$ transition. The coordinates of the triple point are $p_{\text{trp}} = 0.183$ GPa and $T_{\text{trp}} = 199.6$ K. The thermodynamic parameters of the phase transitions at atmospheric and high pressure are listed in the table. The temperature at which the cubic phase loses stability changes with increasing pressure at a very low rate, and the sign reversal of the quantity dT_1/dp is likely to occur, within the accuracy with which this quantity is determined. At the triple point, the G_0 - G_2 phase boundary splits. At pressures above p_{trp} , tungsten oxyfluoride undergoes a sequence of two phase transitions, $G_0 \rightarrow G_3 \rightarrow G_2$. The temperature of the $G_0 \rightarrow G_3$ transformation grows nonlinearly with increasing pressure. The initial shift of the transition temperature occurring at $p = p_{\text{trp}}$ is ~ 435 K/GPa. The G_3 - G_2 phase boundary is linear and has a negative dT/dp coefficient.

The analysis of the DTA data also yielded the values of the enthalpy changes at the phase transitions taking place at high pressure. This was done by subtracting the baseline from the temperature-dependent DTA signal and calculating the area bounded by the anomaly corresponding to the phase transition. The area obtained for the transformation at atmospheric pressure ($G_0 \rightarrow G_2$) in relative units was assumed equal to the enthalpy change $\Sigma\Delta H = 3370$ J/mol (found in heat capacity measurements using adiabatic calorimetry) in the phase transition sequence $G_0 \rightarrow G_1 \rightarrow G_2$. The enthalpy changes in the successive pressure-induced phase transformations $G_0 \rightarrow G_3$ and $G_3 \rightarrow G_2$ were derived from the ratio of the areas bounded by the corresponding DTA peaks (see table). Near the triple point, the relation connecting the enthalpies of these phase transitions, $\Delta H(G_0 \rightarrow G_2) = \Delta H(G_0 \rightarrow G_3) + \Delta H(G_3 \rightarrow G_2)$, should be met. As seen from a comparison of the above data, this relation is satisfied within the error with which the quantities ΔH are determined. The increase in the error of determining ΔH at high pressures originates from the increase in heat losses, which, in turn, is caused by the increase in the thermal conductivity of the pressure-transmitting liquid.

The T vs. p phase diagram of the $(\text{NH}_4)_3\text{TiOF}_5$ oxyfluoride is shown in Fig. 6. Its pattern is more complex than that of the tungsten compound. Two high-pressure

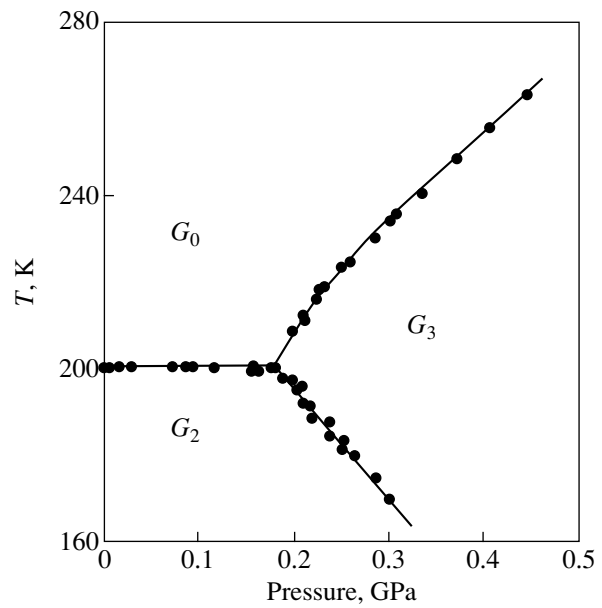


Fig. 5. T vs. p diagram of $(\text{NH}_4)_3\text{WO}_3\text{F}_3$.

phases and two triple points were revealed having the following parameters: $T_{1\text{trp}} = 265.7$ K, $p_{1\text{trp}} = 0.196$ GPa, and $T_{2\text{trp}} = 249.2$ K, $p_{2\text{trp}} = 0.291$ GPa. At the first triple point, the $G_0 \rightarrow G'_1$ phase-transition line splits into two lines, corresponding to the $G_0 \rightarrow G'_2$ and $G'_2 \rightarrow G'_1$ transitions. The latter transition operates within a comparatively narrow pressure interval (approximately 0.1 GPa). At the second triple point, the phase boundaries $G'_2 \rightarrow G'_1$, $G'_2 \rightarrow G'_3$, and $G'_1 \rightarrow G'_3$ terminate. The displacements of all phase transition temperatures identified in the phase diagram of titanium oxyfluoride are presented in the table. The slope of the $G'_1 \rightarrow G'_3$ phase boundary would suggest that this transformation also occurs at atmospheric pressure near 120 K. As follows, however, from our calorimetric measurements (see Section 3), there are no heat capacity anomalies in $(\text{NH}_4)_3\text{TiOF}_5$ in the temperature interval from T_0 to 80 K. Hence, it may be con-

Thermodynamic parameters of the phase transitions in $(\text{NH}_4)_3\text{WO}_3\text{F}_3$ and $(\text{NH}_4)_3\text{TiOF}_5$ revealed by T vs. p diagrams

Phase transition	$(\text{NH}_4)_3\text{WO}_3\text{F}_3$			$(\text{NH}_4)_3\text{TiOF}_5$				
	G_0 - G_2	G_0 - G_3	G_3 - G_2	G_0 - G'_1	G_0 - G'_2	G'_2 - G'_1	G'_2 - G'_3	G'_1 - G'_3
dT/dp , K/GPa	-2.5 ± 5	~ 435	-252 ± 14	6.3 ± 0.5	223 ± 9	-176 ± 12	-59 ± 12	425 ± 17
ΔH , J/mol	3370 ± 250	1000 ± 250	1900 ± 480	4820 ± 720	1320 ± 260	3400 ± 680	5300 ± 1060	1890 ± 380
ΔS , J/mol K	16.9 ± 1.2	5.0 ± 1.3	9.5 ± 2.4	18.1 ± 1.0	5.0 ± 1.0	12.8 ± 2.6	21.3 ± 4.3	7.6 ± 1.5
$\Delta V/V$, %	0.04	1.9	-2.1	0.1	1.0	-2.0	-1.1	2.8

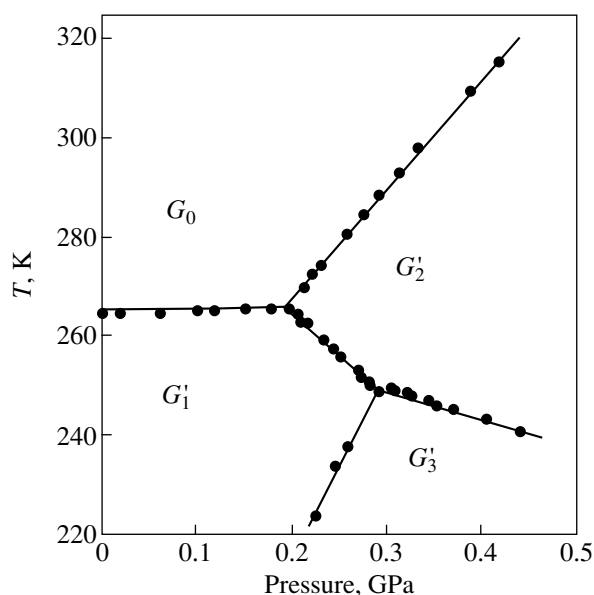


Fig. 6. T vs. p diagram of $(\text{NH}_4)_3\text{TiOF}_5$.

tured that, at pressures below 0.2 GPa, the $G_1' \rightarrow G_3'$ is nonlinear, with rising dT/dp .

We used the method employed earlier to analyze the phase diagram of tungsten oxyfluoride to determine the enthalpy changes characteristic of the structural transformations in the titanium compound (see table). The enthalpies for the corresponding phase transition lines terminating at the triple points agree satisfactorily in relative magnitude within the experimental error.

5. DISCUSSION OF THE RESULTS

Our calorimetric, x-ray diffraction, and DTA measurements performed under pressure revealed phase transitions and pressure-induced phases in the $(\text{NH}_4)_3\text{WO}_3\text{F}_3$ and $(\text{NH}_4)_3\text{TiOF}_5$ ammonium oxyfluorides with cryolite structure. Substitution of the spherical atomic cation by the tetrahedral ammonium cation brought about, as expected, a substantial lowering of the temperature at which the cubic phase loses stability. For instance, the phase transitions from the cubic phase in the $\text{K}_3\text{WO}_3\text{F}_3$ and K_3TiOF_5 compounds take place at 452 K [5] and 490 K [6], respectively, with the simultaneous formation of the ferroelectric and ferroelastic states. In view of the single crystals used here being too small, we did not carry out studies of the permittivity and polarization, which leaves the question of the existence of ferroelectricity in the distorted phases of $(\text{NH}_4)_3\text{WO}_3\text{F}_3$ and $(\text{NH}_4)_3\text{TiOF}_5$ open. Observations performed with a polarization microscope showed that the nature of the structural transformations in both oxyfluorides investigated here is at least ferroelastic.

Although the results of our studies are insufficient to establish the symmetry of the distorted phases, we can

maintain with confidence that the symmetry is different for $(\text{NH}_4)_3\text{WO}_3\text{F}_3$ and $(\text{NH}_4)_3\text{TiOF}_5$, because the latter was found to change translational symmetry at T_0 .

As follows from calorimetric data, the phase transitions detected in our study are first-order transformations. Knowing the ratio between the jump in the entropy and its total change, one can determine the extent to which the transition is close to the tri-critical point. For the $G_0 \rightarrow G_1'$ transformation in titanium oxyfluoride, this ratio is $\delta S_0/\Delta S_0 = 0.84$. The appreciable difference between the values of T_0 and δT_0 for this compound, as determined by DSM and from quasi-static thermograms, clearly indicates a noticeable dependence of the hysteresis phenomena on the temperature scanning rate and also provides supportive evidence of the phase transition being far from the tri-critical point.

The intermediate phase G_1 in $(\text{NH}_4)_3\text{WO}_3\text{F}_3$ exists in a very narrow temperature interval ($T_1 - T_2 = 1.6$ K) and apparently disappears in the T vs. p diagram at low pressures. Therefore, the degree of closeness to the tri-critical point could be estimated only for the $G_0 \rightarrow G_2$ transition by assuming, because the entropy is an additive quantity, that the relation $\delta S(G_0 \rightarrow G_2) = \delta S(G_0 \rightarrow G_1) + \delta S(G_1 \rightarrow G_2)$ is valid. The total latent heat found from the thermograms is $\Sigma \delta H_i = 2700 \pm 150$ J/mol. In defining the entropy jump as $\delta S(G_0 \rightarrow G_2) = \Sigma \delta H_i/T_1$, we found that the $G_0 \rightarrow G_2$ phase transition in this compound is also fairly far from the tri-critical point, $\delta S(G_0 \rightarrow G_2)/\Delta S(G_0 \rightarrow G_2) = 0.8$. We may recall that some ammonium-fluorine cryolites and elpasolites, for instance, $(\text{NH}_4)_3\text{ScF}_6$ [10] and $\text{Cs}_2\text{NH}_4\text{GaF}_6$ [11], likewise exhibit large ratios $\delta S_0/\Delta S_0 = 0.86$.

Using the available information on the entropies of the phase transitions and the displacement of transformation temperatures induced by hydrostatic pressure, we used the Clapeyron–Clausius relation $dT/dp = (\Delta V/V)/\Delta S$ to estimate the relative changes in unit cell volume $\Delta V/V$ at phase transitions in the vicinity of the triple points (see table). Note that the pressure-induced phase transitions in $(\text{NH}_4)_3\text{WO}_3\text{F}_3$ and $(\text{NH}_4)_3\text{TiOF}_5$ are apparently more clearly pronounced first-order transformations, because the unit cell volume change for these compounds is several times larger than $\Delta V/V$ for transitions at atmospheric pressure.

The data listed in the table also suggest that the entropy change for all phase transitions in both ammonium oxyfluorides is typically $\Delta S/R \geq \ln 2$. We can therefore conclude with confidence that the observed structural distortions are associated with the ordering of some structural elements. Note also that the phase transitions $G_0 \rightarrow G_2$ in $(\text{NH}_4)_3\text{WO}_3\text{F}_3$ and $G_0 \rightarrow G_1'$ in $(\text{NH}_4)_3\text{TiOF}_5$ entail the same entropy change $\Delta S/R$ of approximately $\ln 8$, despite the difference in symmetry between the distorted phases. Figure 7 displays the temperature dependence of the excess entropy. As

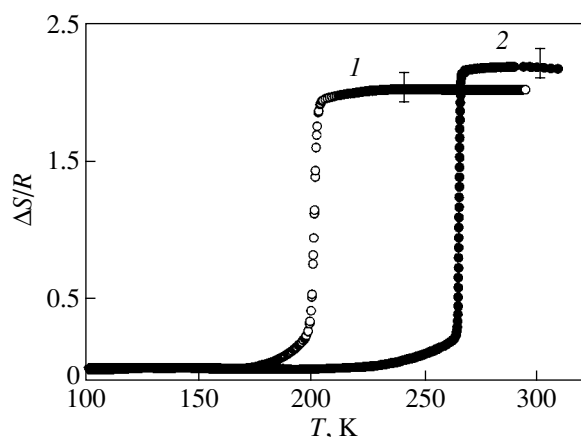


Fig. 7. Temperature dependence of the excess entropy of (1) $(\text{NH}_4)_3\text{WO}_3\text{F}_3$ and (2) $(\text{NH}_4)_3\text{TiOF}_5$. R is the universal gas constant.

shown by DSM studies, the change in entropy observed in a number of tungsten oxyfluorides of cryolite structure with atomic cations is typically $\Delta S/R \leq \ln 2$ [5]. Thus, it is obvious that substitution of tetrahedral for spherical cations brings about a larger disorder in the $Fm\bar{3}m$ cubic structure. On the other hand, phase transitions from the cubic phase occurring in $(\text{NH}_4)_3\text{ScF}_6$ and $\text{Cs}_2\text{NH}_4\text{CaF}_6$ are also accompanied by an entropy change of $\ln 8$ [10, 11]. Such a large value of $\Delta S/R$ was assigned to partial ordering of the $M^{3+}\text{F}_6$ octahedra ($\ln 4$) and ordering of the ammonium tetrahedra in the $4b$ position ($\ln 2$). We do not currently have at our disposal data on the structure of either cubic or distorted phases of $(\text{NH}_4)_3\text{WO}_3\text{F}_3$ and $(\text{NH}_4)_3\text{TiOF}_5$. Therefore, we believe that consideration of any model concepts accounting for the established transition entropies would be premature.

However, the relation between the entropies near the triple points observed in the phase diagrams of both oxyfluorides indicates that the pressure-induced consecutive phase transitions also belong to order-disorder-type transformations.

ACKNOWLEDGMENTS

The authors are grateful to S.V. Mel'nikova for providing results of optical polarization studies.

This study was supported by the Russian Foundation for Basic Research (project nos. 03-02-16079, 03-02-06728, 01-03-32719) and the Department of Physical Sciences of the Russian Academy of Sciences (project no. 2.2.6.1).

REFERENCES

1. I. N. Flerov, M. V. Gorev, K. S. Aleksandrov, A. Tressaud, J. Grannec, and M. Couzi, *Mater. Sci. Eng. R* **24** (3), 81 (1998).
2. G. von Pausewang and W. Rüdorff, *Z. Anorg. Allg. Chem.* **364** (1–2), 69 (1969).
3. K. von Dehnicke, G. Pausewang, and W. Rüdorff, *Z. Anorg. Allg. Chem.* **366** (1–2), 64 (1969).
4. M. Couzi, V. Rodriguez, J.-P. Chaminade, M. Fouad, and J. Ravez, *Ferroelectrics* **80**, 109 (1988).
5. G. Peraudeau, J. Ravez, P. Hagenmüller, and H. Arend, *Solid State Commun.* **27**, 591 (1978).
6. M. Fouad, J. P. Chaminade, J. Ravez, and P. Hagenmüller, *Rev. Chim. Miner.* **24**, 1 (1987).
7. S. C. Abrahams, J. L. Bernstein, and J. Ravez, *Acta Crystallogr. B* **37** (7), 1332 (1981).
8. Z. G. Ye, J. Ravez, J.-P. Rivera, J.-P. Chaminade, and H. Schmid, *Ferroelectrics* **124**, 281 (1991).
9. F. J. Brink, R. L. Withers, K. Friese, G. Madariaga, and L. Noren, *J. Solid State Chem.* **163**, 267 (2002).
10. I. N. Flerov, M. V. Gorev, and T. V. Ushakova, *Fiz. Tverd. Tela (St. Petersburg)* **41** (3), 523 (1999) [*Phys. Solid State* **41**, 468 (1999)].
11. M. V. Gorev, I. N. Flerov, A. Tressaud, A. I. Zaitsev, and E. Durand, *Solid State Sci.* **4** (1), 15 (2002).

Translated by G. Skrebtsov